N-Monoalkylation of Amines with Alcohols by Tandem Photocatalytic and Catalytic Reactions on TiO$_2$ Loaded with Pd Nanoparticles

Yasuhiro Shiraishi,*,[†] Keisuke Fujiwara,[†] Yoshitsune Sugano,[†] Satoshi Ichikawa,[‡] and Takayuki Hirai[†]

[†]Research Center for Solar Energy Chemistry, and Division of Chemical Engineering, Graduate School of Engineering Science, Osaka University, Toyonaka 560-8531, Japan

[‡]Institute for NanoScience Design, Osaka University, Toyonaka 560-8531, Japan

ABSTRACT: TiO$_2$ loaded with Pd particles (Pd/TiO$_2$), when photoirradiated at $\lambda > 300$ nm in alcohol containing primary amine, efficiently promotes N-monoalkylation of amine with alcohol, producing the corresponding secondary amine with almost quantitative yields. This occurs via tandem photocatalytic and catalytic reactions: (i) Pd-assisted alcohol oxidation on the photoactivated TiO$_2$, (ii) condensation of the formed aldehyde with amine on the TiO$_2$ surface, and (iii) hydrogenation of the formed imine by the surface H atoms on the Pd particles. The rate-determining step is the imine hydrogenation, and the reaction depends strongly on the size of the Pd particles. The catalyst with 0.3 wt % Pd, containing 2−2.5 nm Pd particles, shows the highest activity for imine hydrogenation, and smaller or larger Pd particles are inefficient. Calculations of the number of surface Pd atoms based on the cuboctahedron particle model revealed that the Pd atoms on the triangle site of Pd particles are the active site for hydrogenation. Larger Pd particles contain a larger number of these Pd atoms and are effective for imine hydrogenation. Alcohols, however, are strongly adsorbed onto the larger triangle site and suppress imine hydrogenation. As a result of this, the catalyst with 2−2.5 nm Pd particles, which contains a relatively larger number of Pd atoms on the triangle site and does not promote strong alcohol adsorption, shows the highest activity for imine hydrogenation and promotes efficient N-monoalkylation of amine with alcohol under photoirradiation.

KEYWORDS: photocatalysis, titanium dioxide, nanoparticles, palladium, N-alkylation
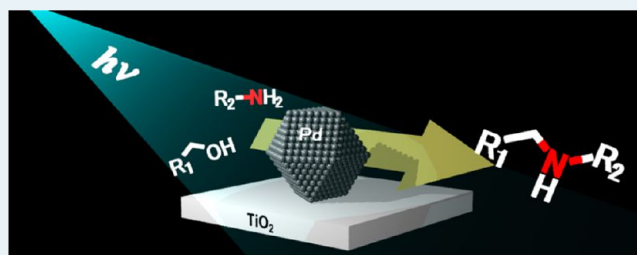
INTRODUCTION

Tandem catalysis that enables multistep reactions in one pot has attracted a great deal of attention because it avoids the isolation of unstable intermediates and reduces the production of wastes.[1−3] A variety of one-pot synthetic procedures have been proposed, but many of these employ homogeneous catalysts, which generally suffer from product contamination and limited recyclability.[4−6] Development of heterogeneous catalytic systems that promote efficient one-pot synthetic reactions is currently the focus of attention.[7−11]

Secondary amines are one of the most important classes of chemicals that are widely used for synthesis of pharmaceuticals and agricultural chemicals.[12] Traditionally, these compounds are synthesized by N-monoalkylation of primary amines with alkyl halides.[12−14] This method, however, requires stoichiometric or excess amounts of inorganic bases, with a concomitant formation of large amounts of inorganic salts as waste.

An alternative environmentally friendly way for secondary amine synthesis is the N-alkylation of primary amines with alcohols as the alkylating reagents in the presence of transition metal catalysts, the so-called "borrowing hydrogen (H) strategy".[15−18] The reaction proceeds via three consecutive catalytic steps in one pot: (i) dehydrogenation of an alcohol initially proceeds, producing aldehyde and H atoms on the metal; (ii) catalytic condensation of the formed aldehyde with primary amine produces imine; and (iii) the imine is hydrogenated by the H atoms, giving the secondary amine. Although many homogeneous catalysts, such as Pt, Ru, and Ir complexes, have been proposed so far,[19−24] these methods have shortcomings in the recovery and reuse of expensive catalysts, the indispensable use of cocatalysts such as bases and stabilizing ligands, or both. The design of easily recyclable heterogeneous catalytic systems is therefore desirable.

Several heterogeneous systems have also been proposed for one-pot secondary amine synthesis, such as Pd oxides supported on Fe$_2$O$_3$,[25] Pd particles supported on boehmite nanofibers,[26] Ag clusters supported on Al$_2$O$_3$ (in the presence of FeCl$_3$·6H$_2$O as a homogeneous Lewis acid),[27] Ru or Cu hydroxide supported on Al$_2$O$_3$,[28−31] Au particles supported on TiO$_2$,[32] and Pd particles supported on MgO.[33] All of these

Table 1. Catalyst Properties and the Results for N-Alkylation of Aniline with Benzyl Alcohol on Various Catalysts under Photoirradiation
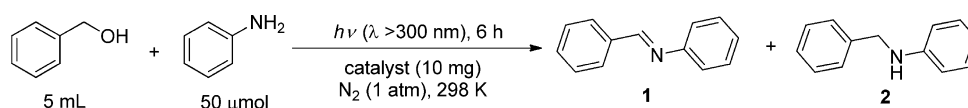
entry	catalyst	d_{pd} (nm)[a]	aniline conv (%)[b]	yields (%)[b,c]		amt product formed (μmol)[b]		
				1	2	benzaldehyde	toluene	H_2
1	TiO_2		11	10	0	<1	0	<1
2	$Au_{0.3}/TiO_2$		4	4	0	16	0	15
3	$Ag_{0.3}/TiO_2$		9	6	2	4	0	3
4	$Pt_{0.3}/TiO_2$		56	53	3	84	0	98
5	$Pd_{0.1}/TiO_2$	1.6	65	8	49	96	0.9	93
6	$Pd_{0.3}/TiO_2$	2.3	>99	6	92	90	14	79
7	$Pd_{0.5}/TiO_2$	2.6	91	9	81	62	25	18
8	$Pd_{1.0}/TiO_2$	4.1	89	19	64	56	42	6
9[d]	$Pd_{0.3}/TiO_2$		>99	7	92			

[a]Average diameter of Pd particles determined by TEM observations (Figure 1). [b]Determined by GC. [c]Yield = [product formed]/[initial amount of aniline] × 100. [d]The result obtained by the reuse of catalyst (entry 6) after simple washing with ethanol.

systems produce secondary amines selectively, but they require relatively high reaction temperatures (>363 K).

The purpose of the present work is to design heterogeneous catalytic systems that promote N-monoalkylation of primary amines with alcohols at room temperature. It is well-known that photoexcitation of semiconductor TiO_2 loaded with noble metal particles, such as Pt,[34] Ag,[35] Au,[36] and Pd,[37] under inert gas atmosphere successfully promotes dehydrogenation of alcohols and produces aldehydes at room temperature. The removed H^+ are reduced by the photoformed electrons on the metal particles and are transformed to H atoms (H−metal species), which are finally removed from the metal surface by the formation of H_2.[38] This indicates that TiO_2 loaded with metal particles, when photoactivated in alcohol, produces aldehyde and H atoms at room temperature. The formed aldehyde may react with primary amine on the Lewis acid site on the TiO_2 surface and produce imine.[34,39] The imine may then be hydrogenated by the H atoms formed on the metal surface[40] and converted to secondary amine.

On the basis of the above scenario, we studied the N-alkylation of primary amines with alcohols in the presence of metal-loaded TiO_2 under photoirradiation (λ > 300 nm). Here, we report that TiO_2 loaded with Pd particles (Pd/TiO_2) successfully promotes N-monoalkylation of primary amines at room temperature via three consecutive steps involving (i) dehydrogenation of alcohols on the photoactivated TiO_2 surface, (ii) catalytic condensation of the formed aldehyde and amine, and (iii) hydrogenation of the formed imine on the Pd surface. We found that the reaction efficiency strongly depends on the size of Pd particles. The catalyst loaded with 0.3 wt % Pd, containing 2−2.5 nm Pd particles, shows the highest activity.

■ **RESULTS AND DISCUSSION**

Catalytic Activity of Metal-Loaded TiO_2. The catalytic activity of metal-loaded TiO_2, M_x/TiO_2 [x (wt %) = M/(M + TiO_2) × 100], was studied for N-alkylation of primary amine with alcohol. The catalysts loaded with 0.3 wt % metal particles such as Au, Pt, Ag, and Pd were prepared with JRC-TIO-4 TiO_2 particles supplied from the Catalyst Society of Japan (equivalent to Degussa P25; anatase/rutile = ~80/20; average particle size, 24 nm; BET surface area, 59 m^2 g^{-1}). Metal

loadings were carried out by the deposition−precipitation method for Au[41] and by the impregnation−reduction method[34] for Pt, Ag, and Pd. These catalysts were used for N-alkylation of aniline with benzyl alcohol. The reactions were carried out by photoirradiation (λ > 300 nm, 6 h) of a benzyl alcohol solution (5 mL) containing aniline (50 μmol) with the respective catalyst (10 mg) at room temperature under N_2 atmosphere (1 atm). The conversion of aniline and the yields of N-benzylidenaniline (1) and N-benzylphenylamine (2) (= [product formed]/[initial amount of aniline] × 100) are summarized in Table 1. With bare TiO_2 (entry 1), the aniline conversion is only 11%, and the imine (1) is formed as the main product, and the secondary amine (2) is scarcely produced. As shown in entries 2 and 3, $Au_{0.3}/TiO_2$ and $Ag_{0.3}/TiO_2$ catalysts are also ineffective; their aniline conversions are <10%. In these cases, the amount of benzaldehyde formed is significantly low (<20 μmol). This implies that photocatalytic oxidation of alcohol does not occur efficiently on these catalysts and does not provide a large enough amount of aldehyde for condensation with aniline. As shown in entry 4, $Pt_{0.3}/TiO_2$ shows a relatively high aniline conversion (56%). The yield of 2, however, is only 3%, and imine (1) is mainly produced. This indicates that hydrogenation of imine does not occur efficiently on the $Pt_{0.3}/TiO_2$ catalyst. In contrast, $Pd_{0.3}/TiO_2$ (entry 6) produces 2 with almost quantitative yield (92%). The results clearly indicate that Pd/TiO_2 catalyst is highly active for N-monoalkylation.

Catalytic Activity of Pd/TiO_2. Pd_x/TiO_2 catalysts with different Pd loadings (x = 0.1, 0.3, 0.5, and 1.0 wt %) were prepared to clarify their activity. Figure 1 shows the typical transmission electron microscopy (TEM) images of catalysts. Highly dispersed Pd nanoparticles were observed for all Pd_x/TiO_2 catalysts. As shown in Figure 1, the size of the Pd particles (d_{Pd}) determined by the TEM observations increases with an increase in the Pd loadings; the average diameters for x = 0.1, 0.3, 0.5, and 1.0 catalysts are 1.6, 2.3, 2.6, and 4.1 nm, respectively. In addition, high-resolution TEM image of catalysts (Figure 2) revealed that the Pd particles can be indexed as fcc in structure, as well as bulk Pd metal (JCPDS 46-1043). Figure 3 shows the diffuse reflectance UV−vis spectra of the respective catalysts. The catalysts with higher Pd loadings
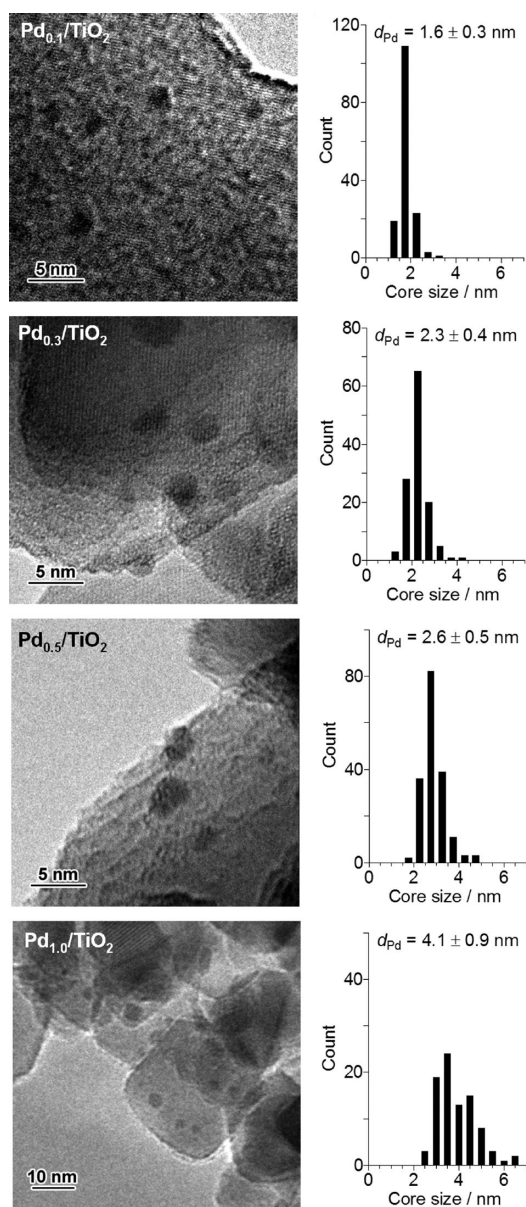
Figure 1. Typical TEM image of Pd_x/TiO_2 catalysts and the size distributions of Pd particles on the respective catalysts.

Figure 2. High-resolution TEM images of Pd_x/TiO_2 catalysts.
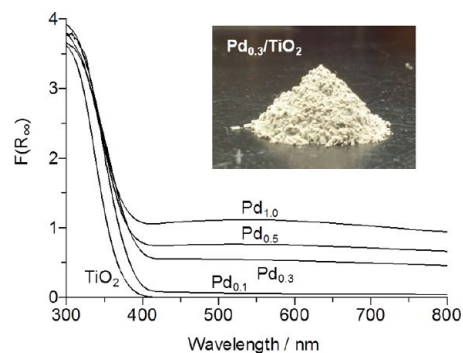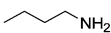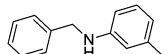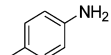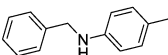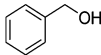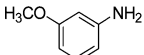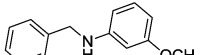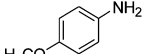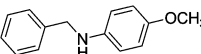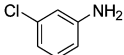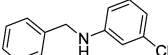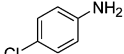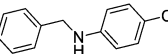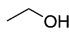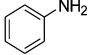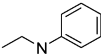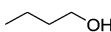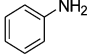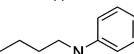
Figure 3. Diffuse reflectance UV−vis spectra of Pd_x/TiO_2 catalysts.

show increased absorbance at $\lambda > 300$ nm due to the light scattering by the Pd particles.

Table 1 (entries 5−8) summarizes the results for N-alkylation of aniline with benzyl alcohol in the presence of Pd_x/TiO_2 catalysts. Among the catalysts, $Pd_{0.3}/TiO_2$ (entry 6) shows the highest aniline conversion (>99%) and the highest **2** yield (92%). The catalysts with lower or higher Pd loadings show decreased activity. These data suggest that $Pd_{0.3}/TiO_2$ shows the best catalytic activity, and the activity strongly depends on the amount of Pd loaded. It is noted that the $Pd_{0.3}/TiO_2$ catalyst is reusable for further reaction. As shown in Table 1 (entry 9), $Pd_{0.3}/TiO_2$, when reused for reaction after simple washing with ethanol, shows aniline conversions and a yield of **2** that are similar to that obtained with the virgin catalyst (entry 6). This indicates that the catalyst is reusable without the loss of activity and selectivity. In addition, $Pd_{0.3}/TiO_2$ is applicable for synthesis of several kinds of secondary amines. As shown in Table 2, photoirradiation of $Pd_{0.3}/TiO_2$ in alkyl or benzyl

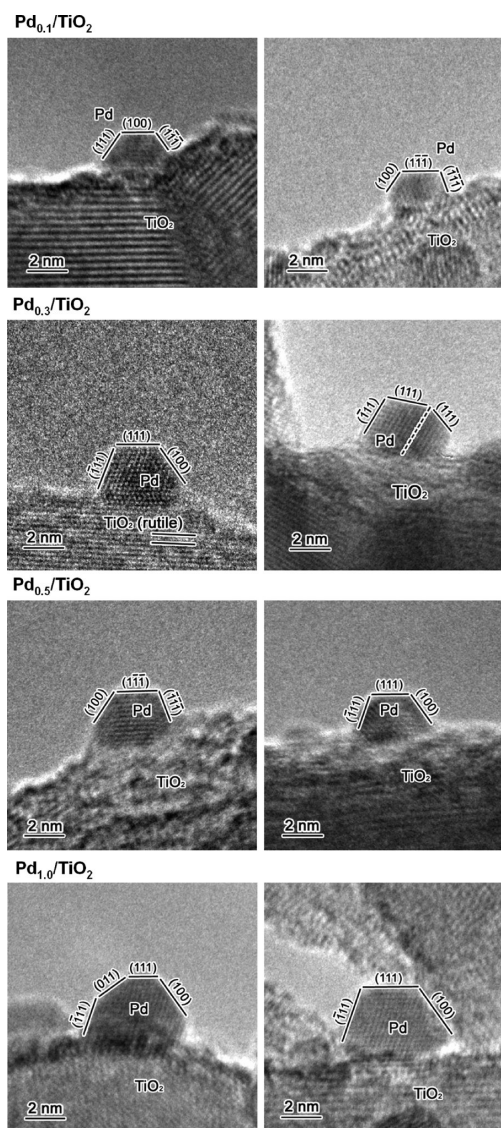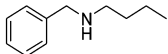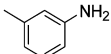alcohols containing several kinds of primary amines produces the corresponding secondary amines with very high yields (>82%).

Mechanism for N-Alkylation. The Pd/TiO_2 catalysts promote N-alkylation of amine with alcohol via tandem photocatalytic and catalytic reactions. The reactions are

Table 2. N-Alkylation of Various Amines with Alcohols on the $Pd_{0.3}/TiO_2$ Catalyst under Photoirradiation[a]

Entry	Alcohol	Amine	t [h]	Amine Conv. [%][b]	Product	Yield [%][b]
1			6	>99		98
2			12	>99		97
3			14	98		82
4			12	>99		96
5			16	94		82
6			12	>99		95
7			12	>99		82
8			3	>99		95
9			4	>99		91

[a]Reaction conditions: alcohol, 5 mL; amine, 50 μmol; catalyst, 10 mg; temperature, 298 K; N_2, 1 atm; λ > 300 nm; [b]Determined by GC.

Figure 4. Time-dependent change in the amounts of substrate and products during photoreaction of benzyl alcohol and aniline with (a) $Pd_{0.1}/TiO_2$, (b) $Pd_{0.3}/TiO_2$, and (c) $Pd_{1.0}/TiO_2$ catalysts. Reaction conditions are identical to those in Table 1.

initiated by photoexcitation of TiO_2, producing the electron (e^-) and positive hole (h^+) pairs.

$$TiO_2 + h\nu \rightarrow h^+ + e^- \tag{1}$$

The h^+ oxidizes alcohol and produces aldehyde and H^+.

$$R_1-CH_2OH + 2h^+ \rightarrow R_1-CHO + 2H^+ \tag{2}$$

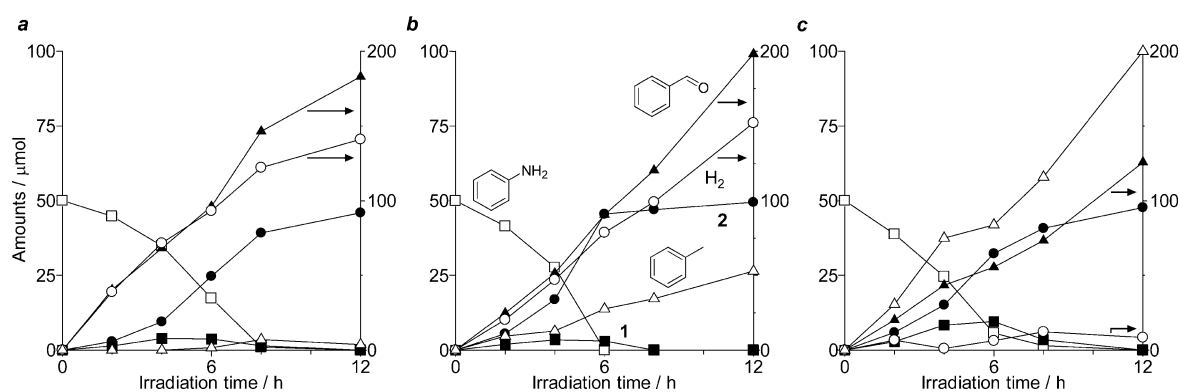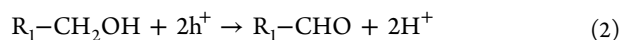H^+ is reduced on the surface of Pd particles by the e^- transferred from the TiO_2 conduction band, and transformed to the surface H atom (H–Pd species).

$$H^+ + e^- + Pd \rightarrow H-Pd \tag{3}$$

Parts of the H atoms are removed from the surface of Pd particles as H_2 gas by coalescence.

$$H-Pd + H-Pd \rightarrow H_2\uparrow + 2Pd \tag{4}$$
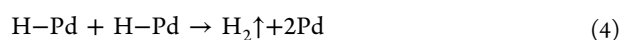
Condensation of the formed aldehyde with primary amine by the Lewis acid site on the TiO_2 surface produces the imine. The reaction occurs reversibly as follows:[34,39]

$$R_1-CHO + R_2-NH_2 \rightleftarrows R_1-CH=N-R_2 + H_2O \tag{5}$$
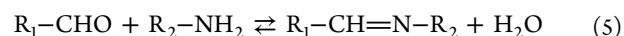
The imine is hydrogenated by the H–Pd species and is transformed to secondary amine.[40]

$$R_1-CH=N-R_2 + 2H-Pd \rightarrow R_1-CH_2-NH-R_2 + 2Pd \tag{6}$$
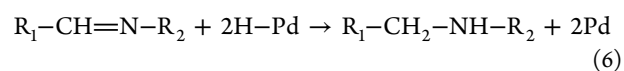
Figure 4 shows the time-dependent change in the amounts of substrate and products during the photocatalytic reaction of aniline with benzyl alcohol in the presence of $Pd_{0.1}/TiO_2$, $Pd_{0.3}/TiO_2$, and $Pd_{1.0}/TiO_2$ catalysts, respectively. As shown in Figure 4b, photoirradiation of $Pd_{0.3}/TiO_2$ produces benzaldehyde and H_2 at the initial stage, then the amount of aniline decreases, and the imine **1** and secondary amine **2** appear. The amount of **1** stays very low, and the amount of **2** increases with time; 6 h of photoirradiation leads to almost quantitative transformation of

aniline to **2**. These substrate and product profiles suggest that the above reaction sequence (eqs 1−6) proceeds efficiently on the $Pd_{0.3}/TiO_2$ catalyst. In contrast, with $Pd_{0.1}/TiO_2$ and $Pd_{1.0}/TiO_2$ (Figure 4a and c), the formation of **2** is much slower than that obtained with $Pd_{0.3}/TiO_2$; quantitative formation of **2** requires more than 10 h. These data suggest that $Pd_{0.3}/TiO_2$ shows the highest activity for N-alkylation, and the amount of Pd loaded strongly affects the catalytic activity.

Effects of Pd Amount on the Reaction Steps. The effects of the Pd amount on the respective reaction steps (eqs 2−6) for N-alkylation were studied to clarify the reason for the high activity of $Pd_{0.3}/TiO_2$. The oxidation of alcohol by the photoformed h^+ (eq 2) as the first step for reaction was studied by photoirradiation of the respective catalysts (10 mg) in benzyl alcohol (5 mL) without aniline. Figure 5 (white) shows

Figure 5. Amount of products formed during photoreaction of benzyl alcohol with respective catalysts in the absence of amine.

the amount of benzaldehyde formed by 6 h of photoirradiation. $Pd_{0.1}/TiO_2$ produces the highest amount of aldehyde, and the amount decreases with the Pd loadings. This suggests that lower Pd loading catalysts are active for photocatalytic oxidation of alcohol. It is well-known that a metal/semiconductor heterojunc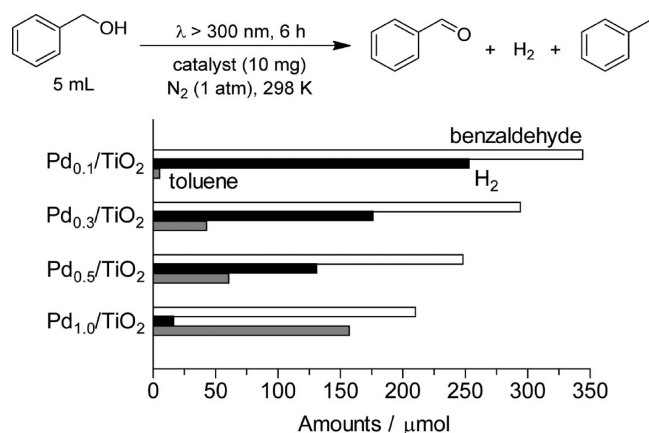tion creates a Schottky barrier.[42] Photoformed conduction band e^- of a semiconductor overcomes this barrier and is trapped by the metal particles, resulting in an enhanced charge separation between h^+ and e^-. The charge separation efficiency therefore strongly depends on the height of the Schottky barrier. The increased metal loadings onto the semiconductor lead to an increase in the height of the Schottky barrier as a result of the electron transfer from the semiconductor to the metal.[43] The increased barrier height by larger Pd loadings probably suppresses the migration of the conduction band e^- to the Pd particles. This may decrease the charge separation efficiency and result in decreased photocatalytic aldehyde formation (Figure 5). However, as shown in Table 1 (entries 5−8), all of the Pd_x/TiO_2 catalysts produce benzaldehyde with amounts larger than that of aniline (50 μmol). This suggests that an amount of aldehyde that is sufficient for condensation with aniline is produced on all of the catalysts, and the photocatalytic alcohol oxidation is not the rate-determining step for N-alkylation.

Condensation of amine with aldehyde (eq 5) is the next step for N-alkylation. The reaction is catalyzed by the Lewis acid site on the TiO_2 surface[34,39] and is not affected by the amount of Pd loaded. Table 3 summarizes the results for condensation between aniline and 2 equiv of benzaldehyde in the presence of

Table 3. Condensation of Benzaldehyde with Aniline on the Respective Catalysts in the Dark.[a]
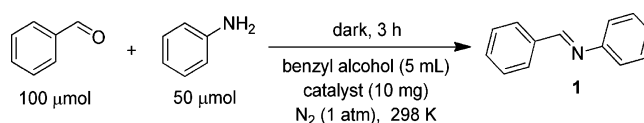
entry	catalyst	1 yield (%)[a]
1	none	29
2	TiO_2	90
3	$Pd_{0.1}/TiO_2$	92
4	$Pd_{0.3}/TiO_2$	94
5	$Pd_{0.5}/TiO_2$	92
6	$Pd_{1.0}/TiO_2$	95

[a]Determined by GC.

the respective catalysts for 3 h at 298 K in the dark. The absence of catalyst (entry 1) produces **1** with only 29% yield. In contrast, addition of bare TiO_2 (entry 2) produces **1** with >90% yield. The yield of **1** scarcely changes when using the catalysts with different Pd loadings (entries 3−6). These data clearly suggest that the imine formation (eq 5) is also not the rate-determining step for N-alkylation.

As a result of the above, the rate-determining step for N-alkylation is the hydrogenation of imine by the H atom formed on the surface of Pd particles (eq 6) as the final step for reaction sequence. The imine hydrogenation is strongly affected by the size of the Pd particles loaded. This is confirmed by hydrogenation of imine **1** with molecular hydrogen (H_2) as a hydrogen source. The reaction was performed in MeCN containing **1** with H_2 (1 atm) in the presence of respective Pd_x/TiO_2 catalysts at a constant Pd amount (0.28 μmol) for 2 h in the dark. Figure 6 (black) shows the relationship between the diameter of Pd particles (d_{Pd}) and the yield of secondary amine (**2**) formed. Smaller Pd particles have a larger surface area and possess a larger number of surface Pd atoms. The **2** yields, however, increase with an increase in the size of the Pd
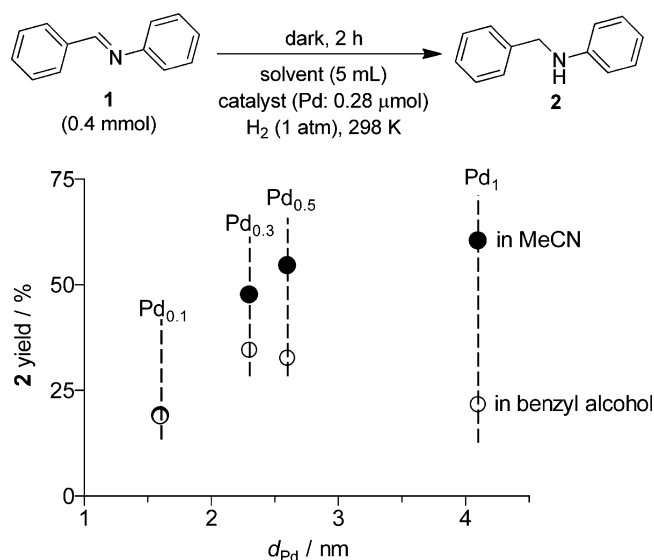

Figure 6. The yields of secondary amine **2** obtained during hydrogenation of imine **1** in MeCN or benzylalcohol with respective Pd_x/TiO_2 catalysts (Pd: 0.28 μmol) under H_2 in the dark. The amounts of catalysts used are 30 ($Pd_{0.1}$), 10 ($Pd_{0.3}$), 6 ($Pd_{0.5}$), and 3 mg (Pd_1), respectively.

particles. This indicates that not all of the surface Pd atoms are the active site, and the Pd atoms on the specific surface site behave as the active site for imine hydrogenation.

Active Site for Imine Hydrogenation. The specific active site for imine hydrogenation on the Pd particles must be identified. Morphology and size of metal particles strongly affect the catalytic activity because of the electronic and geometric effects.[44−47] Metal particles contain different types of surface atoms located at the vertex, edge, square, and triangle sites. The number of these atoms changes substantially with the size of the particles. As shown in Figure 2, high-resolution TEM images of catalysts revealed that the shape of the Pd particle is part of cuboctahedron, which is surrounded by [111] and [100] surfaces. The Pd particles on the TiO_2 surface can therefore simply be modeled as a fcc cuboctahedron, as shown in Figure 7a, which is often used for related nanoparticle systems.[48−50]
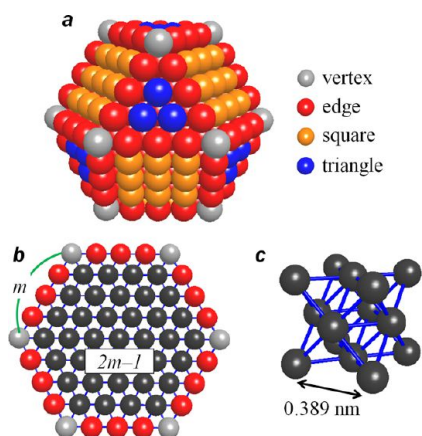

Figure 7. (a) The fcc cuboctahedron model for Pd particles. (b) The largest cross-sectional (111) hexagonal facet of the Pd particle. (c) The unit lattice of Pd particle.

This allows rough determination of the number of Pd atoms on the respective surface sites. Considering the full shell close packing cuboctahedron for the Pd particle where one Pd atom is surrounded by 12 others, the number of total Pd atoms per particle (N_{total}^*) and the number of surface Pd atoms per particle ($N_{surface}^*$) can be expressed by the following equations using the shell number (m).

$$N_{total}^* = \frac{1}{3}(2m - 1)(5m^2 - 5m + 3) \tag{7}$$

$$N_{surface}^* = 10m^2 - 20m + 12$$
$$= N_{vertex}^* + N_{edge}^* + N_{square}^* + N_{triangle}^* \tag{8}$$

The numbers of Pd atoms on the specific surface sites ($N_{specific}^*$) such as vertex, edge, square, and triangle sites per Pd particles are therefore expressed by the following equations.[51]

$$N_{vertex}^* = 12 \tag{9}$$

$$N_{edge}^* = 24(m - 2) \tag{10}$$

$$N_{square}^* = 6(m - 2)^2 \tag{11}$$

$$N_{triangle}^* = 4(m - 3)(m - 2) \tag{12}$$

As shown in Figure 7b, the number of Pd atoms on the diagonal line of the largest cross-sectional (111) facet of Pd

particle is expressed as $2m-1$. The lattice constant of Pd is 0.389 nm (Figure 7c),[52] and the atomic diameter of Pd is 0.274 nm.[53] The diameter of the Pd particle (d_{Pd}) is therefore expressed as follows:

$$d_{Pd}(nm) = \frac{0.389}{\sqrt{2}}\{(2m - 1) - 1\} + 0.274 \tag{13}$$

The number of Pd particles per unit weight of Pd ($n_{particle}$), and the number of Pd atoms on the specific surface site (vertex, edge, square, triangle) per unit weight of Pd ($N_{specific}$) can therefore be expressed using the molecular weight of Pd [M_w (= 106.42 g mol^{-1})], as follows:

$$n_{particle} \ (mol\,g^{-1}) = \frac{1}{M_W \times N_{total}^*} \tag{14}$$

$$N_{specific} \ (mol\,g^{-1}) = N_{specific}^* \times n_{particle} \tag{15}$$

As shown in Figure 1, the average diameters of Pd particles (d_{Pd}) for catalysts were determined by TEM observations to be 1.6 ($Pd_{0.1}/TiO_2$), 2.3 ($Pd_{0.3}/TiO_2$), 2.6 ($Pd_{0.5}/TiO_2$), and 4.1 nm ($Pd_{1.0}/TiO_2$), respectively. The shell numbers (m) for Pd particles on the respective catalysts can therefore be calculated using eq 13. The numbers of Pd atoms on the specific surface site per unit weight of Pd ($N_{specific}$) can then be determined using eqs 9−12, 14, and 15. Figure 8 shows the relationship
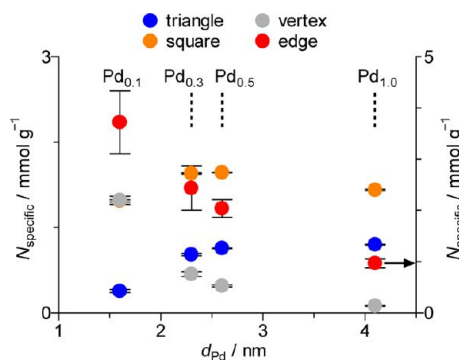
Figure 8. Relationship between the diameter of Pd particles on the respective Pd_x/TiO_2 catalyst and the number of Pd atoms on the specific surface site of the Pd particle per unit weight of Pd.

between the diameter of Pd particles and their respective $N_{specific}$ values. The N_{vertex} and N_{edge} values decrease with an increase in the size of Pd particle, and the N_{square} values scarcely change with the Pd particle size. These profiles are completely different from the catalytic activity of Pd particles for imine hydrogenation (Figure 6, black). In contrast, the $N_{triangle}$ value increases with an increase in the Pd particle size, and the profile is very similar to the imine hydrogenation profile. This calculation result implies that Pd atoms on the triangle site are active for imine hydrogenation.

This is further confirmed by the turnover number for imine hydrogenation per number of Pd atoms on the specific surface site ($TON_{specific}$). The amount of secondary amine **2** (mol) formed during hydrogenation of imine **1** by H_2 with respective Pd_x/TiO_2 catalysts in the dark (Figure 6) was divided by the Pd amount (0.28 μmol) and the respective $N_{specific}$ values, using the following equation:

$$TON_{specific} = \frac{[amount\ of\ product\ formed]}{N_{specific} \times (0.28 \times 10^{-6})} \tag{16}$$

Figure 9 shows the relationship between the size of Pd particle on the catalysts and respective $TON_{specific}$ values. The

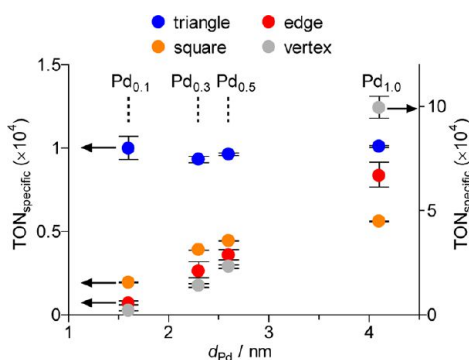**Figure 9.** Relationship between the Pd particle size and the turnover number for hydrogenation of imine **1** per number of Pd atoms on the specific surface site ($TON_{specific}$). The $TON_{specific}$ value was calculated with the results for imine hydrogenation (Figure 6, black) using eq 16.

TON_{vertex}, TON_{edge}, and TON_{square} values change with the Pd particle size. In contrast, the $TON_{triangle}$ values for the respective catalysts are similar and are independent of the Pd particle size. This result clearly indicates that the Pd atoms on the triangle site are the active site for imine hydrogenation.

The H atoms formed on the Pd particles diffuse around the particle surface,[54] meaning that the H atoms exist randomly on all parts of the Pd particle surface. The strong dependence of the imine hydrogenation activity on the number of Pd atoms on the triangle site is probably due to the adsorption of imine onto the triangle site. The Pd atoms on the triangle site have a higher coordination number (9) than those on the other surface sites, such as vertex (5), edge (7), and square (8), and are charged more positively. The imine is therefore preferentially adsorbed onto the positively charged triangle site via π electronic interaction with the aromatic ring and C=N bond. This adsorption may promote efficient hydrogenation by the H−Pd species and result in a clear relationship between the imine hydrogenation activity and the number of Pd atoms on the triangle site. In the hydrogenation of an alkyne and a diene, such as 2-methyl-3-butyn-2-ol[44] and 1,3-butadiene,[55] on Pd particle catalysts with H_2, the catalytic activity also depends on the number of Pd atoms on the triangle site, and the dependence is also considered to be due to the adsorption of these olefins onto the positively charged triangle site. These reports support the above mechanism for imine hydrogenation.

Effect of Alcohol on the Imine Hydrogenation. The above results suggest that the triangle site of Pd particles is the active site for imine hydrogenation. The number of these Pd atoms increases with an increase in the Pd particle size, and the Pd_x/TiO_2 catalyst with higher Pd loadings, which contain larger Pd particles, efficiently promotes imine hydrogenation. However, as shown in Figure 4b and c, photocatalytic reaction of benzyl alcohol and aniline with $Pd_{1.0}/TiO_2$ shows much lower activity for imine hydrogenation than $Pd_{0.3}/TiO_2$. This is inconsistent with the results for imine hydrogenation with H_2 (Figure 6, black).

The lower imine hydrogenation activity of larger Pd particles is because alcohols are adsorbed onto the larger triangle site more strongly than imines and undergo hydrogenation. Figure 6 (white) shows the results for imine hydrogenation with H_2 when carried out in benzyl alcohol. The hydrogenation activity

of smaller Pd particles is similar to that obtained in MeCN (black), but the activity of larger Pd particles is decreased significantly. These data clearly indicate that the imine hydrogenation on larger Pd particles is suppressed by alcohol. In these cases, GC analysis detected the formation of toluene. This indicates that, as reported,[56] Pd particles promote hydrogenation of alcohol by the H−Pd species, leading to hydrogenolysis.

Figure 10a shows the amount of toluene formed during hydrogenation of benzyl alcohol with H_2 in the dark with the
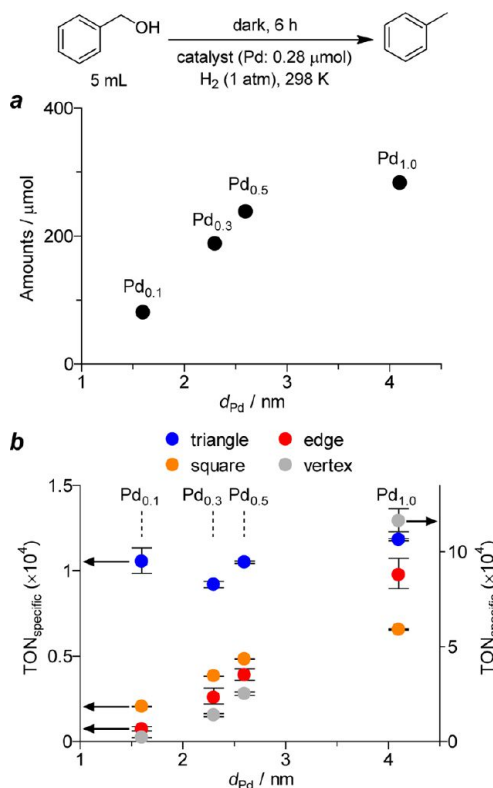

Figure 10. (a) Amount of toluene formed during reaction of benzyl alcohol with respective Pd_x/TiO_2 catalysts (Pd: 0.28 μmol) under H_2 in the dark. The amounts of catalysts used are 30 ($Pd_{0.1}$), 10 ($Pd_{0.3}$), 6 ($Pd_{0.5}$), and 3 mg (Pd_1), respectively. (b) Relationship between the Pd particle size and the turnover number for toluene formation per number of Pd atoms on the specific surface site ($TON_{specific}$). The $TON_{specific}$ values were calculated using eq 16.

respective Pd_x/TiO_2 catalysts at the identical Pd amount (0.28 μmol). The hydrogenation activity increases with the Pd particle size, and the profile is very similar to the imine hydrogenation profile (Figure 6, black). Figure 10b shows the turnover number for toluene formation per number of specific surface sites ($TON_{specific}$) calculated using eq 16. The $TON_{triangle}$ values for all of the catalysts are similar, as is the case for imine hydrogenation (Figure 9). These findings indicate that the hydrogenation of alcohol is also promoted on the triangle site of Pd particles, and this suppresses the imine hydrogenation.

The strongly suppressed imine hydrogenation on larger Pd particles is probably due to the stronger adsorption of alcohol than imine onto larger triangle site by their different adsorption modes. As shown in Figure 11, benzyl alcohol has a planar structure and is adsorbed very strongly onto the Pd surface via π interaction of the aromatic ring and the lone pair electron of
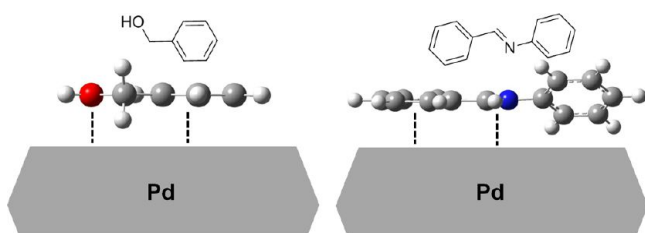
Figure 11. Schematic representation of different adsorption modes of benzyl alcohol and imine **1** onto the surface of a Pd particle. Geometry optimizations of the molecules were performed with B3LYP/6-31G* basis set.

the oxygen atom.[57] In contrast, the imine has a twisted structure[58] and may be adsorbed more weakly onto the Pd surface. The interaction between alcohol and the Pd surface is probably strengthened by an increase in the area of the triangle site. This probably leads to enhanced alcohol adsorption onto the larger Pd particles and suppresses imine hydrogenation more strongly. As shown in Figures 4 and 5, a larger amount of toluene is produced during the photocatalytic reaction of alcohol in the presence of catalysts with a larger Pd particle. This indicates that the decreased imine hydrogenation activity of larger Pd particles is due to the strong adsorption of alcohols. These results suggest that the $Pd_{0.3}/TiO_2$ catalyst with 2−2.5 nm Pd particles, which contains a relatively larger number of triangle site Pd atoms but does not allow strong adsorption of alcohols, shows the highest activity for imine hydrogenation and promotes efficient N-monoalkylation of primary amine with alcohol under photoirradiation.

CONCLUSION

We found that Pd/TiO_2 catalyst promotes N-monoalkylation of primary amine with alcohol under photoirradiation at room temperature. Several kinds of secondary amines are successfully produced with high yields. Tandem photocatalytic and catalytic reactions promote three consecutive reactions, consisting of Pd-assisted alcohol oxidation on the photoactivated TiO_2, catalytic condensation of the formed aldehydes with amines on the TiO_2 surface, and hydrogenation of formed imine with H atoms on the Pd particles. The rate-determining reaction is the imine hydrogenation as the final step. The reaction is promoted on the Pd atoms on the triangle site of the Pd particle via an adsorption of imine. The imine adsorption onto the larger triangle site is strongly suppressed by competitive adsorption of alcohol. As a result of this, the catalyst with 2−2.5 nm Pd particles, which contain a relatively larger number of triangular Pd atoms and do not promote strong alcohol adsorption, shows the highest activity for imine hydrogenation and promotes efficient N-alkylation of amine with alcohol under photo-irradiation. This tandem catalytic system offers significant advantages: (i) no harmful byproduct forms, (ii) the reaction proceeds at room temperature, and (iii) several secondary amines are successfully produced. The tandem reactions promoted by photocatalytic and catalytic actions, therefore, have a potential to be a powerful method for one-pot synthesis of organic compounds in an environmentally friendly way.

EXPERIMENTAL SECTION

Materials. All reagents were purchased from Wako, Tokyo Kasei, and Sigma-Aldrich and were used without further

purification. Japan Reference Catalyst JRC-TIO-4 TiO_2 particles were kindly supplied by the Catalysis Society of Japan.

Pd_x/TiO_2 [x (wt %) = 0.1, 0.3, 0.5, and 1.0] were prepared as follows: TiO_2 (1.0 g) and $Pd(NO_3)_2$ (2.2, 6.5, 10.9, or 21.9 mg) were added to water (40 mL) and evaporated under vigorous stirring at 353 K for 12 h. The obtained powders were calcined at 673 K under air flow (0.5 L min^{-1}) and then reduced at 673 K under H_2 flow (0.2 L min^{-1}). The heating rate and holding time at 673 K for these treatments were 2 K min^{-1} and 2 h, respectively. $Ag_{0.3}/TiO_2$ and $Pt_{0.3}/TiO_2$ were prepared in a manner similar to those for Pd_x/TiO_2, using $AgNO_3$ (4.7 mg), or $H_2PtCl_6 \cdot 6H_2O$ (8.0 mg) as precursor.

$Au_{0.3}/TiO_2$ was prepared by a deposition-precipitation method as follows: $HAuCl_4 \cdot 4H_2O$ (6.3 mg) was added to water (50 mL). The pH of the solution was adjusted to 7 by an addition of 1 M NaOH. TiO_2 (1.0 g) was added, and the solution was stirred vigorously at 353 K for 3 h. The solids were recovered by centrifugation and washed with water. The obtained solids were dried at 353 K and calcined at 673 K for 2 h under air flow (0.5 L min^{-1}).

Photoreaction. Each of the respective catalysts (10 mg) was suspended in alcohol (5 mL) containing a required amount of amine within a Pyrex glass tube (ϕ, 10 mm; capacity, 20 mL). The tube was sealed with a rubber septum cap. The catalyst was dispersed by ultrasonication for 5 min, and N_2 was bubbled through the solution for 5 min. The tube was photoirradiated with magnetic stirring at 298 K by a 2 kW Xe lamp ($\lambda > 300$ nm; Ushio Inc.). The light intensity at 300−400 nm is 18.2 W m^{-2}. After photoirradiation, the gas-phase product was analyzed by GC/TCD (Shimadzu; GC-8A). The resulting solution was recovered by centrifugation and analyzed by GC/FID (Shimadzu; GC-1700), and the substrate and product concentrations were determined with authentic samples. Identification of the products was performed by a Shimadzu GC/MS system (GCMS-QP5050A).

Hydrogenation by H_2. Each of the respective catalysts was suspended in a solution (5 mL) containing substrate within a Schlenk tube. The catalyst was dispersed by ultrasonication for 5 min, and H_2 was bubbled through the solution for 5 min. The H_2 pressure was maintained at 1 atm using a balloon. The tube was placed on the digitally controlled water bath with magnetic stirring at 298 K.

Analysis. Total Pd amounts of the catalysts were determined by an X-ray fluorescence spectrometer (Seiko Instruments, Inc.; SEA2110). Diffuse reflectance UV−vis spectra were measured on an UV−vis spectrophotometer (Jasco Corp.; V-550 with Integrated Sphere Apparatus ISV-469) with $BaSO_4$ as a reference.[59,60] TEM observations were carried out using an FEI Tecnai G2 20ST analytical electron microscope operated at 200 kV.[61] The cuboctahedron Pd particles were created on the Crystal Studio Ver. 9.0 software (CrystalSolf. Inc.) and used for calculation of the number of Pd atoms.[50] Ab initio calculations were carried out with the Gaussian 03 program, and the geometry optimization was performed with the density functional theory (DFT) using the B3LYP function with the 6-31G* basis set.[62,63]

AUTHOR INFORMATION

Corresponding Author
*E-mail: shiraish@cheng.es.osaka-u.ac.jp.

Notes
The authors declare no competing financial interest.

REFERENCES

(1) Lee, J. M.; Na, Y.; Han, H.; Chang, S. *Chem. Soc. Rev.* **2004**, *33*, 302−312.
(2) Kolb, H. C.; VanNieuwenhze, M. S.; Sharpless, K. B. *Chem. Rev.* **1994**, *94*, 2483−2547.
(3) Wasilke, J.-C.; Obrey, S. J.; Baker, R. T.; Bazan, G. C. *Chem. Rev.* **2005**, *105*, 1001−1020.
(4) Gunanathan, C.; Ben-David, Y.; Milstein, D. *Science* **2007**, *317*, 790−792.
(5) Cadierno, V.; Francos, J.; Gimeno, J.; Nebra, N. *Chem. Commun.* **2007**, 2536−2538.
(6) Zweifel, T.; Naubron, J.-V.; Grützmacher, H. *Angew. Chem., Int. Ed.* **2009**, *48*, 559−563.
(7) Yin, L.; Liebscher, J. *Chem. Rev.* **2007**, *107*, 133−173.
(8) Motokura, K.; Fujita, N.; Mori, K.; Mizugaki, T.; Ebitani, K.; Kaneda, K. *J. Am. Chem. Soc.* **2005**, *127*, 9674−9675.
(9) Felpin, F.-X.; Fouquet, E. *ChemSusChem* **2008**, *1*, 718−724.
(10) Kim, J. W.; Yamaguchi, K.; Mizuno, N. *Angew. Chem., Int. Ed.* **2008**, *47*, 9249−9251.
(11) Shiraishi, Y.; Sugano, Y.; Tanaka, S.; Hirai, T. *Angew. Chem., Int. Ed.* **2010**, *49*, 1656−1660.
(12) Salvatore, R. N.; Yoon, C. H.; Jung, K. W. *Tetrahedron* **2001**, *57*, 7785−7811.
(13) Buchwald, S. L.; Mauger, C.; Mignani, G.; Scholz, U. *Adv. Synth. Catal.* **2006**, *348*, 23−39.
(14) Navarro, O.; Marion, N.; Mei, J.; Nolan, S. P. *Chem.—Eur. J.* **2006**, *12*, 5142−5148.
(15) Hamid, M. H. S. A.; Slatford, P. A.; Williams, J. M. J. *Adv. Synth. Catal.* **2007**, *349*, 1555−1575.
(16) Guillena, G.; Ramón, D. J.; Yus, M. *Chem. Rev.* **2010**, *110*, 1611−1641.
(17) Guillena, G.; Ramón, D. J.; Yus, M. *Angew. Chem., Int. Ed.* **2007**, *46*, 2358−2364.
(18) Nixon, T. D.; Whittlesey, M. K.; Williams, J. M. J. *Dalton Trans.* **2009**, 753−762.
(19) Tsuji, Y.; Takeuchi, R.; Ogawa, H.; Watanabe, Y. *Chem. Lett.* **1986**, *15*, 293−294.
(20) Watanabe, Y.; Tsuji, Y.; Ohsugi, Y. *Tetrahedron Lett.* **1981**, *22*, 2667−2670.
(21) Naskar, S.; Bhattacharjee, M. *Tetrahedron Lett.* **2007**, *48*, 3367−3370.
(22) Fujita, K.; Enoki, Y.; Yamaguchi, R. *Tetrahedron* **2008**, *64*, 1943−1954.
(23) Blank, B.; Madalska, M.; Kempe, R. *Adv. Synth. Catal.* **2008**, *350*, 749−758.
(24) Michlik, S.; Kempe, R. *Chem.—Eur. J.* **2010**, *16*, 13193−13198.
(25) Zhang, Y.; Qi, X.; Cui, X.; Shi, F.; Deng, Y. *Tetrahedron Lett.* **2011**, *52*, 1334−1338.
(26) Kwon, M. S.; Kim, S.; Park, S.; Bosco, W.; Chidrala, R. K.; Park, J. *J. Org. Chem.* **2009**, *74*, 2877−2879.
(27) Shimizu, K.; Nishimura, M.; Satsuma, A. *ChemCatChem* **2009**, *1*, 497−503.
(28) Yamaguchi, K.; Mizuno, N. *Synlett* **2010**, *16*, 2365−2382.
(29) Kim, J. W.; Yamaguchi, K.; Mizuno, N. *J. Catal.* **2009**, *263*, 205−208.
(30) Yamaguchi, K.; He, J.; Oishi, T.; Mizuno, N. *Chem.—Eur. J.* **2010**, *16*, 7199−7207.
(31) He, J.; Yamaguchi, K.; Mizuno, N. *Chem. Lett.* **2010**, *39*, 1182−1183.
(32) He, L.; Lou, X.-B.; Ni, J.; Liu, Y.-M.; Cao, Y.; He, H.-Y.; Fan, K.-N. *Chem.—Eur. J.* **2010**, *16*, 13965−13969.
(33) Corma, A.; Ródenas, T.; Sabater, M. J. *Chem.—Eur. J.* **2010**, *16*, 254−260.
(34) Shiraishi, Y.; Ikeda, M.; Tsukamoto, D.; Tanaka, S.; Hirai, T. *Chem. Commun.* **2011**, *47*, 4811−4813.
(35) Sclafani, A.; Mozzanega, M.-N.; Pichat, P. *J. Photochem. Photobiol., A* **1991**, *59*, 181−189.
(36) Bamwenda, G. R.; Tsubota, S.; Nakamura, T.; Haruta, M. *J. Photochem. Photobiol., A* **1995**, *89*, 177−189.
(37) Ohtani, B.; Kakimoto, M.; Nishimoto, S.; Kagiya, T. *J. Photochem. Photobiol., A* **1993**, *70*, 265−272.
(38) Shiraishi, Y.; Takeda, Y.; Sugano, Y.; Ichikawa, S.; Tanaka, S.; Hirai, T. *Chem. Commun.* **2011**, *47*, 7863−7865.
(39) Jennings, W. B.; Lovely, C. J. *Tetrahedron* **1991**, *47*, 5561−5568.
(40) Krupka, J.; Patera, J. *Appl. Catal., A* **2007**, *330*, 96−107.
(41) Tsukamoto, D.; Shiraishi, Y.; Sugano, Y.; Ichikawa, S.; Tanaka, S.; Hirai, T. *J. Am. Chem. Soc.* **2012**, *134*, 6309−6315.
(42) Schottky, W. *Z. Phys.* **1939**, *113*, 367−414.
(43) Uchihara, T.; Matsumura, M.; Yamamoto, A.; Tsubomura, H. *J. Phys. Chem.* **1989**, *93*, 5870−5874.
(44) Semagina, N.; Renken, A.; Laub, D.; Kiwi-Minsker, L. *J. Catal.* **2007**, *246*, 308−314.
(45) Bars, J.; Le.; Specht, U.; Bradlay, J. S.; Blackmond, D. G. *Langmuir* **1999**, *15*, 7621−7625.
(46) Coq, B.; Figueras, F. *J. Mol. Catal. A: Chem.* **2001**, *173*, 117−134.
(47) Molnár, A.; Sárkány, A.; Varga, M. *J. Mol. Catal. A: Chem.* **2001**, *173*, 185−221.
(48) Wilson, O. M.; Knecht, M. R.; Garcia-Martinez, J. C.; Crooks, R. M. *J. Am. Chem. Soc.* **2006**, *128*, 4510−4511.
(49) Arruda, T. M.; Shyam, B.; Zeigelbauer, J. M.; Mukerjee, S.; Ramaker, D. E. *J. Phys. Chem. C* **2008**, *112*, 18087−18097.
(50) Shiraishi, Y.; Tsukamoto, D.; Sugano, Y.; Shiro, A.; Ichikawa, S.; Tanaka, S.; Hirai, T. *ACS Catal.* **2012**, *2*, 1984−1992.
(51) Benfield, R. E. *J. Chem. Soc. Faraday Trans.* **1992**, *88*, 1107−1110.
(52) Fornander, H.; Hultman, L.; Birch, J.; Sundgren, J.-E. *J. Cryst. Growth* **1998**, *186*, 189−202.
(53) Pauling, L. *J. Am. Chem. Soc.* **1947**, *69*, 542−553.
(54) Parambhath, V. B.; Nagar, R.; Sethupathi, K.; Ramaprabhu, S. *J. Phys. Chem. C* **2011**, *115*, 15679−15685.
(55) Silvestre-Albero, J.; Rupprechter, G.; Freund, H. J. *Chem. Commun.* **2006**, 80−82.
(56) Keresszegi, C.; Ferri, D.; Mallat, T.; Baiker, A. *J. Phys. Chem. B* **2005**, *109*, 958−967.
(57) Souto, R. M.; Rodríguez, J. L.; Pastor, E. *Langumuir* **2000**, *16*, 8456−8462.
(58) Traetteberg, M.; Hilmo, I. *J. Mol. Struct.* **1978**, *48*, 395−405.
(59) Shiraishi, Y.; Saito, N.; Hirai, T. *J. Am. Chem. Soc.* **2005**, *127*, 8304−8306.
(60) Shiraishi, Y.; Saito, N.; Hirai, T. *J. Am. Chem. Soc.* **2005**, *127*, 12820−12822.
(61) Tsukamoto, D.; Shiro, A.; Shiraishi, Y.; Sugano, Y.; Ichikawa, S.; Tanaka, S.; Hirai, T. *ACS Catal.* **2012**, *2*, 599−603.
(62) Shiraishi, Y.; Ichimura, C.; Sumiya, S.; Hirai, T. *Chem.—Eur. J.* **2011**, *17*, 8324−8332.
(63) Shiraishi, Y.; Sumiya, S.; Hirai, T. *Chem. Commun.* **2011**, *47*, 4953−4955.